

Modeling of Large Simple Shear Using a Viscoplastic Overstress Model and Classical Plasticity Model with Different Objective Stress Rates

Özgen Ü. ÇOLAK

*Department of Mechanical Engineering,
Yıldız Technical University, İstanbul-TURKEY
e-mail: colako@alum.rpi.edu*

Received 03.05.2002

Abstract

Large simple shear deformation, which is usually used to test the applicability of various models, is studied by applying the classical plasticity model and the viscoplasticity theory based on overstress (VBO) with the logarithmic stress rate. Hypo-elastic, elastic-perfectly plastic, elastic-plastic linear kinematic and isotropic hardening models are employed. In addition to the logarithmic rate, the influences of the convected Truesdell and co-rotational Jaumann and Green-Naghdi rates on stress-strain behavior in simple shear are investigated. It is observed that unlike the Jaumann rate the logarithmic rate does not exhibit any oscillatory response. The responses of the logarithmic rate to every type of model discussed here are acceptable except the elastic-perfectly plastic case. The finite viscoplasticity theory based on overstress, which has been developed by Krempl and co-workers, with zero isotropic stress rate and non-zero hardening modulus and elastic-plastic kinematic hardening model give the same results at a rate of $10^{-5}1/s$. It is shown that elastic-perfectly plastic, and elastic-plastic kinematic hardening can be modeled with FVBO.

Key words: Objective stress rates, Classical plasticity models, Viscoplasticity, Simple shear

Introduction

Choosing a suitable objective stress rate for the hypo-elastic and the hypo-elastic-plastic models is an important issue. Since the observation of unaccepted oscillatory shear stress response by Dienes (1979), and Nagtegaal and de Jong (1982), a number of different stress rates has been introduced by different investigators. Generally, the objective stress rates can be classified as co-rotational rates (Jaumann, Green-Naghdi, Logarithmic rate etc.) and convected rates (Truesdell, Cotter/ Rivlin and Oldroyd rate). Dienes (1979) noted that when the Jaumann rate is used in the linear hypo-elastic constitutive equation, an oscillatory shear stress response is obtained in finite simple shear. Similar to the case of hypo-elasticity, an oscillatory response was obtained in finite plasticity for linear kinematic hardening (Nagte-

gaal and de Jong, 1982). Dafalias (1985) showed that stress oscillations generated by simple shear with linear kinematic hardening and the Jaumann rate fade away with increasing strain by using the Armstrong-Frederick model. It is also reported by Nagtegaal and De Jong (1982) that oscillation is not experienced for isotropic hardening. Green and Naghdi (1965) obtained a non oscillatory solution to the simple shear problem by using a different objective rate called the Green-Naghdi rate.

Recently a new spin tensor called logarithmic spin and a new objective rate, the logarithmic rate, was introduced by Xiao *et al.* (1997a). It is proven that an objective, co-rotational rate of the logarithmic strain $\ln \mathbf{V}$ is identical to the stretching tensor \mathbf{D} and \mathbf{D} and $\ln \mathbf{V}$ are the only pair with such a property within the family of co-rotational rates; see Bruhns *et al.* (1999) and Xiao *et al.* (1997a and

1997b).

This paper is arranged as follows: in section 2, the convected stress rates, the Truesdell, Cotter-Rivlin, Oldroyd rates, and the co-rotational rates, the Jaumann, Green-Naghdi and logarithmic stress rates, are reviewed. In section 3, a classical plasticity model with various material laws (hypo-elastic, elastic-perfectly plastic, elastic-plastic linear kinematic and isotropic hardening) is given. Then in section 4, in addition to classical plasticity models, the finite viscoplasticity theory based on overstress (FVBO) is introduced and applied to simple shear. At the end, the simulation results for simple shear are given and compared.

Objective Stress Rates

One of the fundamental principles that all constitutive equations have to satisfy is the principle of objectivity or frame indifference. According to this principle, constitutive equations must be invariant under a change of reference frame. Tensor rates used in constitutive equations need to be objective. A co-rotational objective rate of a tensor \mathbf{A} is denoted by

$$\overset{\circ}{\mathbf{A}} = \dot{\mathbf{A}} + \mathbf{A}\boldsymbol{\Omega} - \boldsymbol{\Omega}\mathbf{A} \quad (1)$$

where $\dot{\mathbf{A}}$ is the material rate with respect to the basis of \mathbf{A} . $\overset{\circ}{\mathbf{A}}$ is objective rate of \mathbf{A} and $\boldsymbol{\Omega}$ is a skew-symmetric spin tensor. Later various forms of $\boldsymbol{\Omega}$ will be evaluated.

Co-Rotational rates

A well-known objective rate is the Jaumann rate. It is the obtained by setting $\boldsymbol{\Omega} = \mathbf{W}$ in Equation 1. \mathbf{W} is the anti-symmetric part of the velocity gradient tensor \mathbf{L} , which is defined as $\mathbf{L} = \dot{\mathbf{F}}\mathbf{F}^{-1}$. The Jaumann rate is

$$\overset{\circ}{\boldsymbol{\sigma}} = \dot{\boldsymbol{\sigma}} + \boldsymbol{\sigma}\mathbf{W} - \mathbf{W}\boldsymbol{\sigma} \quad (2)$$

where $\boldsymbol{\sigma}$ is the Cauchy stress tensor.

Another co-rotational stress rate, the Green-Naghdi (1965) rate, is obtained by taking $\boldsymbol{\Omega} = \dot{\mathbf{R}}\mathbf{R}^T$,

$$\overset{\circ}{\boldsymbol{\sigma}} = \dot{\boldsymbol{\sigma}} + \boldsymbol{\sigma}(\dot{\mathbf{R}}\mathbf{R}^T) - (\dot{\mathbf{R}}\mathbf{R}^T)\boldsymbol{\sigma} \quad (3)$$

Recently, Xiao *et al.*, (1997a) proved that the logarithmic rate of the Eulerian logarithmic strain measure, $\ln\mathbf{V}$, is equal to the rate of deformation tensor,

\mathbf{D} . Among the co-rotational rates, only this pair has this property. They introduced a new spin tensor called logarithmic spin, or simply log spin. The logarithmic spin tensor $\boldsymbol{\Omega} = \boldsymbol{\Omega}^{\log}$ is given by

$$\boldsymbol{\Omega}^{\log} = \mathbf{W} + \mathbf{N}^{\log} \quad (4)$$

and

$$\mathbf{N}^{\log} = \begin{cases} 0, & b_1 = b_2 = b_3 \\ \nu[\mathbf{BD}], & b_1 \neq b_2 = b_3 \\ \nu_1[\mathbf{BD}] + \nu_2[\mathbf{B}^2\mathbf{D}] + \nu_3[\mathbf{B}^2\mathbf{DB}], & b_1 \neq b_2 \neq b_3 \end{cases} \quad (5)$$

where

$$\nu = \frac{1}{b_1 - b_2} \left(\frac{1 + (b_1/b_2)}{1 - (b_1/b_2)} + \frac{2}{\ln(b_1/b_2)} \right) \quad (6)$$

and b_i are the eigenvalues of left Cauchy-Green tensor, $\mathbf{B} = \mathbf{F}\mathbf{F}^T$.

$$\nu_k = -\frac{1}{\Delta} \sum_{i=1}^3 (-b_i)^{3-k} \left(\frac{1 + \varepsilon_i}{1 - \varepsilon_i} + \frac{2}{\ln \varepsilon_i} \right), \quad k = 1, 2, 3 \quad (7)$$

$$\varepsilon_1 = b_2/b_3 \quad \varepsilon_2 = b_3/b_1 \quad \varepsilon_3 = b_1/b_2 \quad (8)$$

$$\Delta = (b_1 - b_2)(b_2 - b_3)(b_3 - b_1) \quad (9)$$

The following notation is used:

$$\begin{aligned} [\mathbf{B}^r \mathbf{D} \mathbf{B}^s] &= \mathbf{B}^r \mathbf{D} \mathbf{B}^s - \mathbf{B}^s \mathbf{D} \mathbf{B}^r, \quad [\mathbf{B}^r \mathbf{D}] = \mathbf{B}^r \mathbf{D} - \mathbf{D} \mathbf{B}^r \\ [\mathbf{BD}] &= \mathbf{B} \mathbf{D} - \mathbf{D} \mathbf{B}, \quad r, s = 0, 1, 2 \end{aligned} \quad (10)$$

Convected rates

The convected rates are the Truesdell, Oldroyd and Cotter/Rivlin rates. The Truesdell stress rate, see Truesdell (1955), is defined as

$$\overset{\circ}{\boldsymbol{\tau}} = \dot{\boldsymbol{\tau}} - \mathbf{L}\boldsymbol{\tau} - \boldsymbol{\tau}\mathbf{L}^T \quad (11)$$

where $\boldsymbol{\tau}$ is the Kirchhoff stress tensor, $\boldsymbol{\tau} = \boldsymbol{\sigma}J$, $J = \det(\mathbf{F})$ and $\boldsymbol{\sigma}$ is the Cauchy stress tensor. The upper (u) and lower (l) Oldroyd rates (Oldroyd, 1950) are based on the Cauchy stress tensor and not on the Kirchhoff stress used in the Truesdell rate:

$$\begin{aligned} \overset{\circ}{\boldsymbol{\sigma}}_u &= \mathbf{F}(\overline{\mathbf{F}^{-1}\dot{\boldsymbol{\sigma}}\mathbf{F}^{-T}})\mathbf{F}^T = \dot{\boldsymbol{\sigma}} - \mathbf{L}\boldsymbol{\sigma} - \boldsymbol{\sigma}\mathbf{L}^T \\ \overset{\circ}{\boldsymbol{\sigma}}_L &= \dot{\boldsymbol{\sigma}} + \mathbf{L}^T\boldsymbol{\sigma} - \boldsymbol{\sigma}\mathbf{L} \end{aligned} \quad (12)$$

The Cotter-Rivlin rate, see Cotter and Rivlin (1955), is defined as

$$\overset{\circ}{\boldsymbol{\sigma}} = \mathbf{F}^{-T}(\overline{\mathbf{F}^T\dot{\boldsymbol{\sigma}}\mathbf{F}})\mathbf{F}^{-1} = \dot{\boldsymbol{\sigma}} + \boldsymbol{\sigma}\mathbf{L} + \mathbf{L}^T\boldsymbol{\sigma} \quad (13)$$

Hypo-Elastic and Hypoelastic-Plastic Constitutive Model at Finite Deformation

Hypo-elastic model

The simplest constitutive equation for isotropic hypo-elasticity is

$$\overset{\circ}{\boldsymbol{\sigma}} = \lambda \text{tr}(\mathbf{D})\mathbf{I} + 2G\mathbf{D} \quad (14)$$

where λ and G are Lamé constants, and $\overset{\circ}{\boldsymbol{\sigma}}$ is an objective stress rate.

Hypo-elastic-plastic models

The additive decomposition of the rate of deformation tensor \mathbf{D} is used for modeling the finite elastic-plastic deformation. In this theory, the rate of deformation \mathbf{D} , which is the measure of the stretching is decomposed into the elastic and plastic parts.

$$\mathbf{D} = \mathbf{D}^e + \mathbf{D}^p \quad (15)$$

The von Mises yield criterion is used for modeling rate-independent plasticity with isotropic and kinematic hardening; see Eterovic and Bathe (1990).

Hypo-elastic-plastic model with kinematic hardening:

The kinematic hardening model assumes that the yield surface translates as a rigid body during plastic deformation. Rate independent plasticity with kinematic hardening depends on the set $\{\sigma_y, \boldsymbol{\alpha}\}$ of internal variables. $\boldsymbol{\alpha}$ is a second order tensor known as kinematic or back stress. In plasticity, it is the repository for the Bauschinger effect. Geometrically, the back stress represents the center of the yield surface. Physically it is the resistance to slip and results from the interaction of dislocation with other dislocations and grain boundaries. The von Mises yield criterion, which defines the boundary of the elastic region, is widely used in the modeling of material behavior. The quadratic yield function is written as

$$\mathbf{f} = \frac{3}{2}(\boldsymbol{\sigma}' - \boldsymbol{\alpha}) : (\boldsymbol{\sigma}' - \boldsymbol{\alpha}) - \sigma_y^2 \leq 0 \quad (16)$$

where $\boldsymbol{\sigma}'$ and $\boldsymbol{\alpha}$ are the deviatoric parts of Cauchy stress tensor and back stress tensor respectively, σ_y is initial yield stress in uniaxial tension.

$$\boldsymbol{\sigma}' = \boldsymbol{\sigma} - \frac{1}{3}(\boldsymbol{\sigma} : \mathbf{I})\mathbf{I} \quad (17)$$

Inelastic deformation occurs when the effective stress exceeds the yield stress. The effective stress tensor, \mathbf{s} , is the difference between the applied stress and the back stress tensors and is defined as

$$\mathbf{s} = \boldsymbol{\sigma}' - \boldsymbol{\alpha} \quad (18)$$

The effective stress invariant is given by

$$\bar{s} = \sqrt{\frac{3}{2}\mathbf{s} : \mathbf{s}} \quad (19)$$

The unit normal to the yield surface is

$$\boldsymbol{\chi} = \sqrt{\frac{3}{2}}\frac{\mathbf{s}}{\bar{s}} \quad (20)$$

The effective plastic strain rate is defined as

$$\dot{e}^p = \sqrt{\frac{2}{3}\mathbf{D}^p : \mathbf{D}^p} \quad (21)$$

The flow rule, which is the plastic part of the rate of deformation, is

$$\mathbf{D}^p = \sqrt{\frac{3}{2}} \dot{\epsilon}^p \boldsymbol{\chi} \quad (22)$$

The evolution equation for back stress for linear kinematic hardening is given by

$$\dot{\boldsymbol{\alpha}} = \frac{2}{3} H \mathbf{D}^p \quad (23)$$

Hypo-elastic-plastic model with isotropic hardening: For modeling isotropic hardening, the von Mises yield criterion is used. The evolution of yield surface occurs by its changing size, not by translation of its center. Therefore in isotropic hardening the back stress, $\boldsymbol{\alpha}$, which represents the translation of yield surface, is zero. The yield stress is given as (Johnson and Bammann. 1984)

$$\dot{\sigma}_y = H \dot{\epsilon}^p \quad (24)$$

Hypo-elastic-perfectly plastic model: In this case, there is no isotropic or kinematic hardening, and so the hardening modulus $H = 0$. This yields to a constant yield stress and zero back stress.

Finite Viscoplasticity Theory Based on Overstress (FVBO)

VBO is a unified state variable theory without a yield surface and loading/unloading condition and was developed by Krempl and co-workers; see Krempl (1998), Colak and Krempl (2002a), (2002b). There is no separation of creep and plasticity in the model. It consists of two tensor valued and one scalar state variables with a growth law. A tensor valued kinematic stress is introduced to model the Bauehinger effect. It also sets the tangent modulus at the maximum strain of interest. Another tensor valued state variable is equilibrium stress, which is the rate-independent contribution to hardening. The isotropic stress A is a scalar state variable for modeling rate independent cyclic hardening (or softening) behavior. Its effect is similar to the isotropic hardening in rate-independent plasticity; see Krempl (1996).

FVBO is obtained by replacing the ordinary time derivative by an objective one in the small deformation viscoplasticity theory based on overstress. The flow law for finite deformation theory of VBO is

$$\mathbf{d} = \mathbf{d}^e + \mathbf{d}^p = \frac{1 + \nu}{E} \dot{\mathbf{s}} + \frac{3}{2} \frac{\mathbf{s} - \mathbf{g}}{Ek[\Gamma]} \quad (25)$$

where \mathbf{s} and \mathbf{d} are the deviators of Cauchy stress tensor, $\boldsymbol{\sigma}$ and the rate of deformation tensor \mathbf{D} , respectively, \mathbf{g} is the deviatoric part of equilibrium stress, which is the stress that the material can sustain at rest. E is the Young modulus, ν is the elastic Poisson's ratio. $k = k[\Gamma]$ is a decreasing positive viscosity function and Γ is the overstress invariant with the dimension of stress, defined by

$$\Gamma^2 = \frac{3}{2} (\mathbf{s} - \mathbf{g}) : (\mathbf{s} - \mathbf{g}) \quad (26)$$

The viscosity function is

$$k = k_1 \left[1 + \frac{\Gamma}{k_2} \right]^{-k_3} \quad (27)$$

where k_1 , k_2 and k_3 are material constants.

The equilibrium stress is similar to the back stress in rate-independent plasticity models, but not exactly the same. In the plasticity models, the back stress is considered the repository for kinematic hardening. However, in VBO the equilibrium stress is not. The repository for kinematic hardening is the kinematic stress. The equilibrium stress is introduced to represent the defect structure of the material. It can neither be measured experimentally like other state variables nor controlled. It is the stress that should be overcome in order to generate the inelastic deformation. The growth law for the equilibrium stress is

$$\dot{\mathbf{g}} = \frac{\psi[\Gamma]}{E} \left(\dot{\mathbf{s}} + \frac{\mathbf{s} - \mathbf{g}}{k} - \frac{\Gamma}{k} \frac{(\mathbf{g} - \mathbf{f})}{A} \right) + \left(1 - \frac{\psi[\Gamma]}{E} \right) \dot{\mathbf{f}} \quad (28)$$

where ψ is the shape function that affects the transition between initial quasi-elastic behavior and inelastic flow. It is given by

$$\psi[\Gamma] = C_1 + \frac{C_2 - C_1}{\exp[C_3 \Gamma]} \quad (29)$$

where C_1, C_2 and C_3 are material constants.

During the deformation, on the one hand, the material can harden because of the interaction of the dislocations with others and grain boundaries, and,

on the other hand, recovery can occur when the dislocations with opposite Burger vectors come across and cancel each other. To simulate this behavior, recovery and hardening, the hardening terms, which are the first two terms in the evolution equation of the equilibrium stress and dynamic recovery term, the third term in Equation (28) are included in the evolution equation of the equilibrium stress tensor.

The tensor valued state variable, kinematic stress, \mathbf{f} is given as follows:

$$\overset{\circ}{\mathbf{f}} = \frac{E_t}{E} \frac{(\mathbf{s} - \mathbf{g})}{k[\Gamma]} \quad (30)$$

where E_t is the tangent modulus at the maximum inelastic strain.

The isotropic stress A is the rate independent stress. The growth law, see Colak and Krempl (2000), is given by

$$\dot{A} = A_c[A_f - A]\dot{\epsilon}^p \quad (31)$$

where A_c and A_f are material constants. For cyclic neutral behavior, the isotropic stress is constant ($A_c = 0$). If the initial value of the isotropic stress is less than the final value, cyclic hardening is modeled. The effective inelastic strain rate $\dot{\epsilon}^p$ is defined as

$$\dot{\epsilon}^p = \frac{\Gamma}{Ek} \quad (32)$$

Hypoelastic and Hypoelastic-Plastic with Kinematic Hardening Solutions for Simple Shear Deformation

In simple shear, the motion is described by

$$\begin{aligned} x &= X + \gamma Y \\ y &= Y \\ z &= Z \end{aligned} \quad (33)$$

where γ is shear strain. The associated deformation and velocity gradient tensors are

$$\mathbf{F} = \begin{bmatrix} 1 & \gamma & 0 \\ 0 & 1 & 0 \\ 0 & 0 & 1 \end{bmatrix} \quad \mathbf{L} = \begin{bmatrix} 0 & \dot{\gamma} & 0 \\ 0 & 0 & 0 \\ 0 & 0 & 0 \end{bmatrix} \quad (34)$$

The rate of deformation tensor \mathbf{D} and spin tensor \mathbf{W} are

$$\mathbf{D} = \frac{1}{2} \begin{bmatrix} 0 & \dot{\gamma} & 0 \\ \dot{\gamma} & 0 & 0 \\ 0 & 0 & 0 \end{bmatrix} \quad \mathbf{W} = \frac{1}{2} \begin{bmatrix} 0 & \dot{\gamma} & 0 \\ -\dot{\gamma} & 0 & 0 \\ 0 & 0 & 0 \end{bmatrix} \quad (35)$$

Since $\det(\mathbf{F}) = 1$, the Kirchoff stress is equal to the Cauchy stress.

Elastic case

The elastic solutions are obtained by substituting Equations (33)-(34) into the appropriate stress rate equations given by Equations (2)-(3)-(11)-(12)-(13) and solving the resulting differential equations.

Truesdell Rate

For the Truesdell rate, the resulting differential equations are

$$\begin{aligned} \dot{\sigma}_{11} - 2\dot{\gamma}\sigma_{12} &= 0 \\ \dot{\sigma}_{12} - \dot{\gamma}\sigma_{22} &= \dot{\gamma}\mu \\ \dot{\sigma}_{22} &= 0 \end{aligned} \quad (36)$$

The solution is

$$\sigma_{11} = \gamma^2\mu, \quad \sigma_{12} = \gamma\mu, \quad \sigma_{22} = 0 \quad (37)$$

where μ is the shear modulus, which is defined as $\mu = E / 2(1 + \nu)$, ν is Poisson's ratio and γ is the shear strain. Initial conditions are $\sigma_{11} = \sigma_{12} = \sigma_{22} = 0$ and the shear strain $\gamma = 0$ at time $t = 0$. This solution does not exhibit oscillatory behavior.

Since $\text{tr}(\mathbf{D}) = 0$ in simple shear, the Truesdell and the upper Oldroyd rate give the same results.

Cotter-Rivlin Rate

Examining the simple shear response for the Cotter/Rivlin rate, the results are

$$\begin{aligned} \dot{\sigma}_{22} + 2\dot{\gamma}\sigma_{12} &= 0 \\ \dot{\sigma}_{12} - \dot{\gamma}\mu + \sigma_{11}\dot{\gamma} &= 0 \\ \dot{\sigma}_{11} &= 0 \end{aligned} \quad (38)$$

which can be integrated to yield

$$\sigma_{11} = 0, \quad \sigma_{12} = \gamma\mu, \quad \sigma_{22} = -\gamma^2\mu \quad (39)$$

where the same initial conditions are used as before and no oscillations are found.

Jaumann Rate

For the Jaumann rate, the differential equations are

$$\begin{aligned} \dot{\sigma}_{11} - \dot{\gamma}\sigma_{12} &= 0 \\ \dot{\sigma}_{22} + \dot{\gamma}\sigma_{12} &= 0 \\ \dot{\sigma}_{12} - \dot{\gamma}\mu + \frac{1}{2}\dot{\gamma}(\sigma_{11} - \sigma_{22}) &= 0 \end{aligned} \quad (40)$$

with the solution

$$\sigma_{12} = \sin(\gamma)\mu\sigma_{11} = -\sigma_{22} = \mu(1 - \cos\gamma) \quad (41)$$

Numerical Results

The VBO consists of stiff nonlinear ordinary differential equations. Stiffness implies that a small change in the input may result in large changes in the output. The system of stiff differential equations is numerically integrated using a commercial ordinary differential equation solver program, DGEAR of IMSL.

Simple shear is analyzed with various hardening laws and objective stress rates. The system of differential equations is solved for elastic and elastic-perfectly plastic, elastic-plastic isotropic, linear kinematic hardening and VBO models with the Jaumann, Green-Naghdi, logarithmic and Truesdell rates.

In the first part of this section the simulation results of the classical plasticity models (hypo-elastic, elastic-perfectly plastic, elastic-linear kinematic hardening, isotropic hardening) were given. In the second part, the responses of the FVBO under simple shear are depicted for the following cases: constant isotropic stress and nonzero kinematic stress, variable isotropic stress and zero kinematic stress, constant isotropic stress and zero kinematic stress. At the end, the simulation results of FVBO and classical plasticity approaches are compared and discussed.

Simulation of the behavior of classical plasticity models for simple shear

The behavior of a hypothetical material under simple shear is investigated using the classical plasticity models with various objective stress rates. The material constants used for hypo-elastic and hypo-elastic-plastic models are given in Table 1.

Elastic

The resulting shear and normal stress versus shear strain curves are depicted in Figure 1 and 2 respectively. An oscillatory response in the shear

and normal stress components is observed with the Jaumann rate. Linear behavior in the shear stress and nonlinear behavior in the normal stress are observed for the Truesdell rate. It is seen from Figure 2 that the normal stresses increase nonlinearly for the logarithmic and the Green-Naghdi rates and have essentially the same characteristic.

Table 1. Material constants for hypo-elastic and elastic-plastic models.

Yield stress	$\sigma_y = 180$ MPa
Young Modulus	$E = 195000$ MPa
Poisson's ratio	$\nu = 0.3$
Hardening modulus	$H=2000$ MPa
Material parameter	$c_r = 0.866$

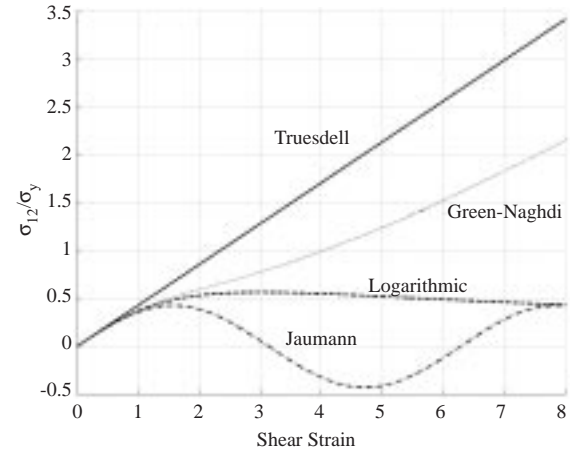


Figure 1. Shear stress vs shear strain: Hypo-elastic material.

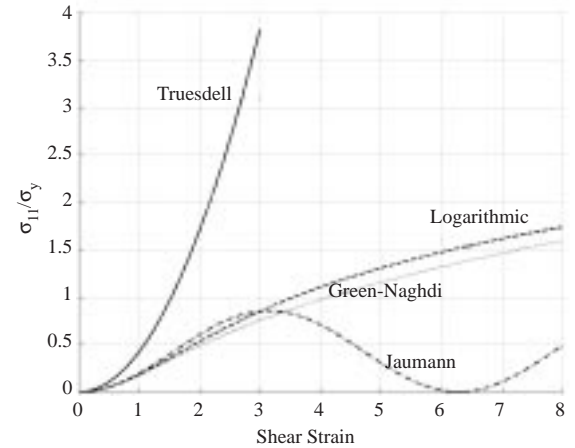


Figure 2. Normal stress vs shear strain: Hypo-elastic material.

Elastic-perfectly plastic

In Figure 3 and 4, the simulation results of the elastic-perfectly plastic model are depicted. A steady state behavior in shear is obtained for all investigated stress rates. The Truesdell and Jaumann rates exhibit perfectly elastic-plastic behavior for the normal stress at different stress levels while the logarithmic and Green-Naghdi rates cause a drop in the normal stress component.

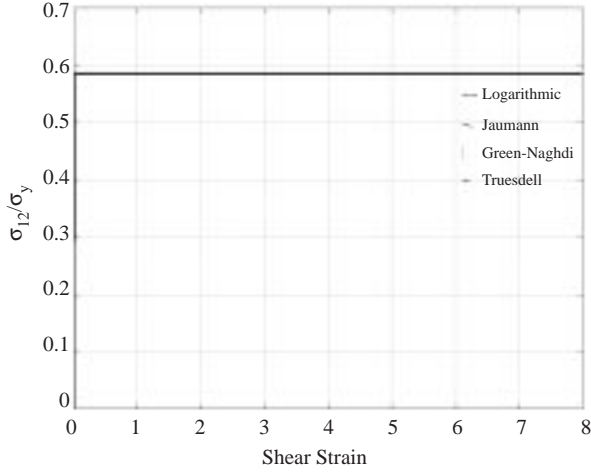


Figure 3. Shear stress vs shear strain: Elastic-perfectly plastic.

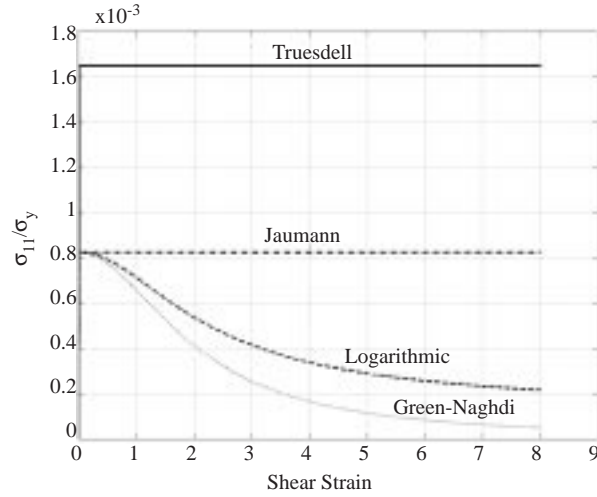


Figure 4. Normal stress vs shear strain: Elastic-perfectly plastic.

Elastic-plastic isotropic hardening

For the elastic-plastic isotropic hardening model, all objective rates investigated exhibit the same linear characteristic in shear stress (Figure 5). Since

the size of the yield surface, which is represented by the yield strength, continues to grow as a function of the effective inelastic strain rate $\dot{\epsilon}^p$ during the deformation, see Equations (21) and (24), the shear and normal stresses continue to increase (Figures 5 and 6). Solutions for isotropic hardening give a nonlinearly increasing normal stress for the Truesdell, logarithmic and Jaumann rates. On the other hand, the normal stress increases nonlinearly and levels off for the Green-Naghdi rate.

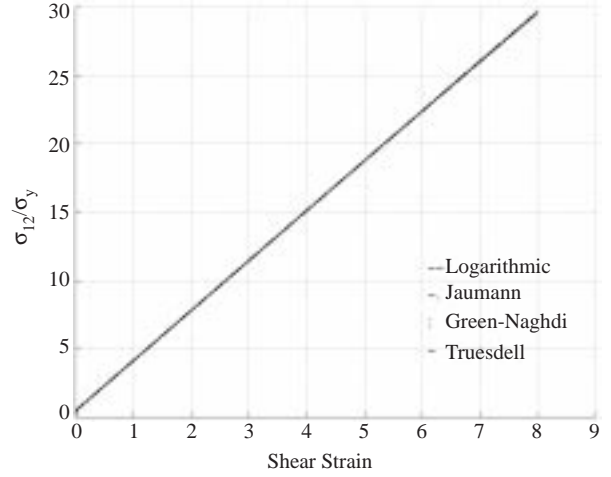


Figure 5. Shear stress vs shear strain: Elastic-plastic with isotropic hardening.

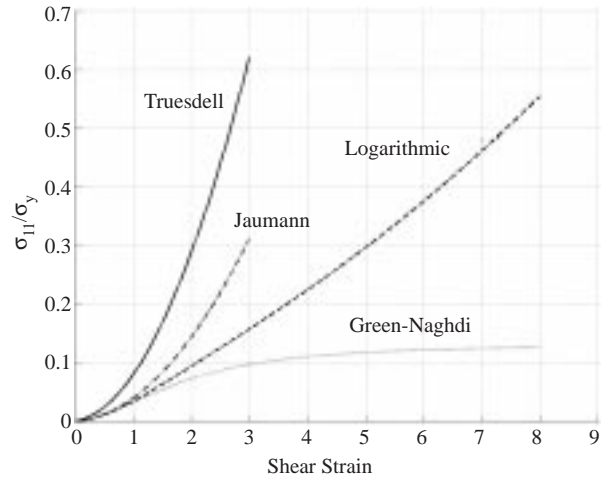


Figure 6. Normal stress vs shear strain: Elastic-plastic with isotropic hardening.

Elastic-plastic kinematic hardening

The simulation results of simple shear for an elastic-plastic linear kinematic hardening material are shown in Figures 7 and 8. An oscillating be-

havior is observed for the Jaumann rate in the case of elastic-plastic linear kinematic hardening.

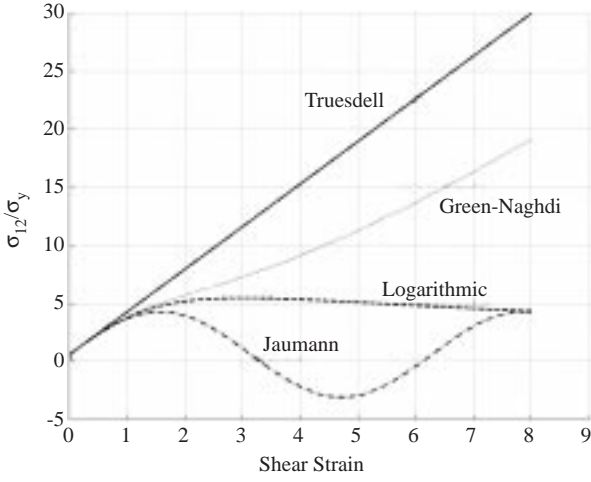


Figure 7. Shear stress vs shear strain: Elastic-plastic with linear kinematic hardening.

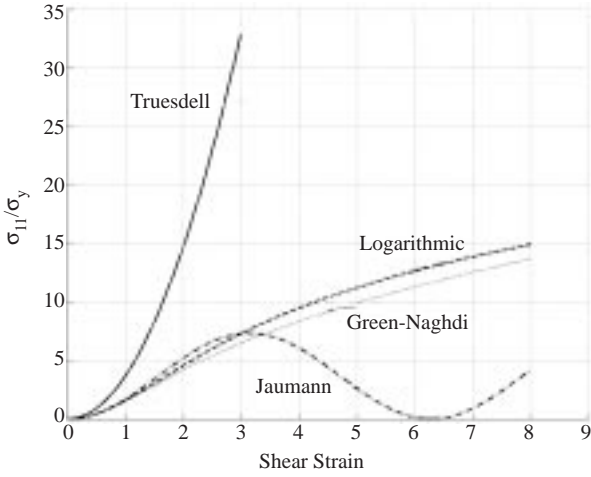


Figure 8. Normal stress vs shear strain: Elastic-plastic with kinematic hardening.

Simulation of the behavior of FVBO for simple shear

The material behavior under simple shear is investigated using FVBO with the convected Truesdell rate and three co-rotational rates: the Jaumann, Green-Naghdi and logarithmic rates. The simulation results of FVBO under simple shear are depicted for the following cases:

- i. Constant isotropic stress ($A = 149$ MPa) and zero kinematic stress ($E_t = 0$) to model elastic-perfectly plastic material behavior. The

stress-strain diagram obtained with the elastic-perfectly plastic model under uniaxial loading is depicted in Figure 9. In addition, the simulation behavior of VBO with constant isotropic stress and zero kinematic stress is shown in the same figure. The elastic-perfectly plastic model and VBO with the parameters mentioned above yields the same results except the transition from the quasi-elastic to fully plastic region.

- ii. Constant isotropic stress ($A = 149$ MPa) and nonzero kinematic stress ($E_t \neq 0$), (Table 2). The stress-strain diagrams under uniaxial loading for kinematic hardening using the classical plasticity model and VBO with constant isotropic stress and nonzero tangent modulus are shown in Figure 10. Similar to the elastic-perfectly plastic case, curves match in the inelastic region.
- iii. Variable isotropic stress, see Equation. (31) and Table 2, and zero kinematic stress ($E_t = 0$) to model isotropic hardening.

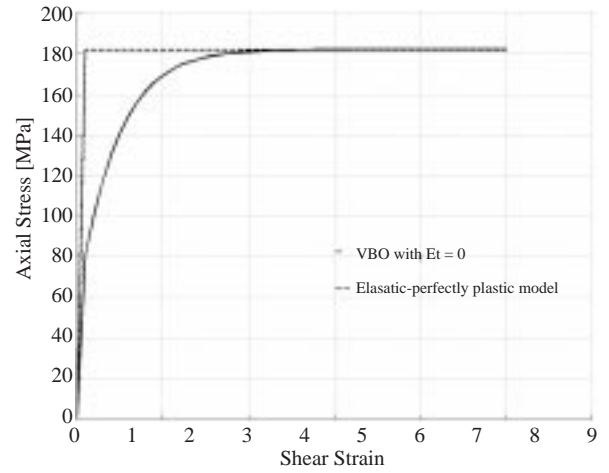


Figure 9. The stress-strain diagrams under uniaxial loading using FVBO with a constant isotropic stress ($A = 149$ MPa) and $E_t = 0$ and the elastic-perfectly plastic model.

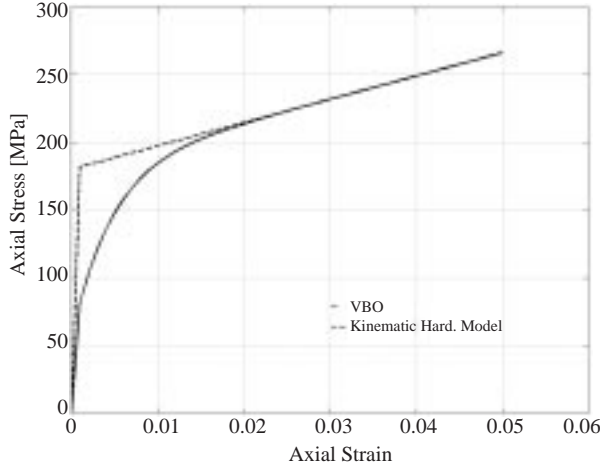


Figure 10. The stress-strain diagrams under uniaxial loading using FVBO with a constant isotropic stress ($A = 149$ MPa) and $E_t = 2000$ MPa and the elastic-plastic kinematic hardening model.

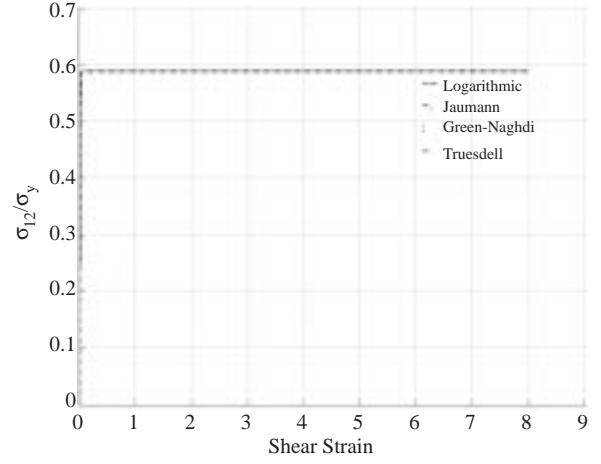


Figure 11. Shear stress vs shear strain: FVBO with zero isotropic stress rate and $E_t = 0$.

Table 2. Material constants for FVBO.

Modulus	$E = 195000$ MPa $E_t = 2000$ MPa $\nu = 0.3$
Isotropic stress	$A_c = 1$ $A_o = 115$ MPa $A_f = 160$ MPa
Viscosity function	$k_1 = 314200$ s $k_2 = 60$ MPa $k_3 = 21.98$
Shape function	$C_1 = 30000$ MPa $C_2 = 182500$ MPa $C_3 = 0.11$ MPa $^{-1}$

For the modeling of elastic-perfectly plastic material behavior with the FVBO the repository for kinematic hardening should be set to zero. In addition, the repository for isotropic hardening should be constant. In FVBO, the tensor valued kinematic stress \mathbf{f} and the scalar isotropic stress A are responsible for kinematic and isotropic hardening, respectively. By setting the hardening modulus E_t to zero and using constant isotropic stress, elastic-perfectly plastic behavior is modeled and the simulation results are shown in Figures 11 and 12. The elastic-perfectly plastic model and FVBO give the same results except the normal stress levels (Figures 3 and 4). The material properties used for FVBO are given in Table 2.

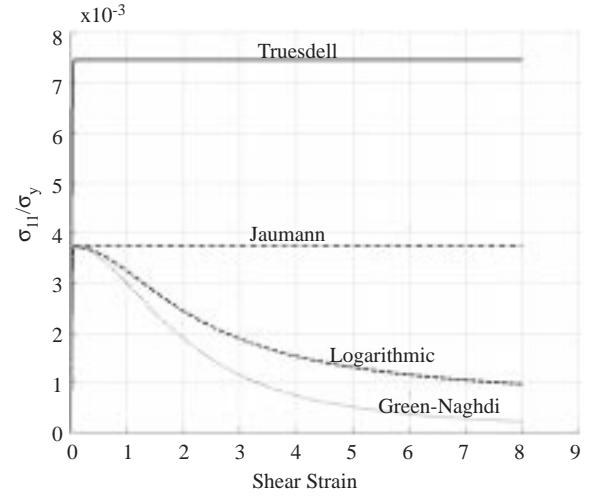


Figure 12. Normal stress vs shear strain: FVBO with zero isotropic stress rate and $E_t = 0$.

A constant isotropic stress and a nonzero hardening modulus yield kinematic hardening. A constant isotropic stress, $A = 149$ MPa is chosen to match the numerical results of FVBO with the classical plasticity model with kinematic hardening. The results of FVBO with constant isotropic stress and non zero kinematic stress are given in Figures. 13 and 14. At a shear strain rate of $10^{-5}1/s$, FVBO and the elastic-plastic linear kinematic hardening model give the same results, (Figures 7 and 8).

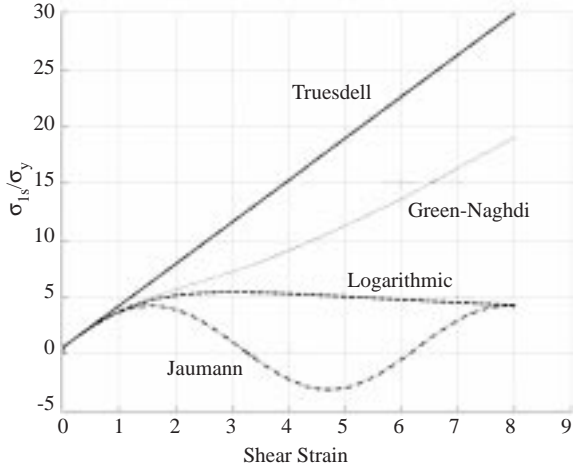


Figure 13. Shear stress vs shear strain: FVBO with zero isotropic stress rate and $E_t = 2000$ MPa.

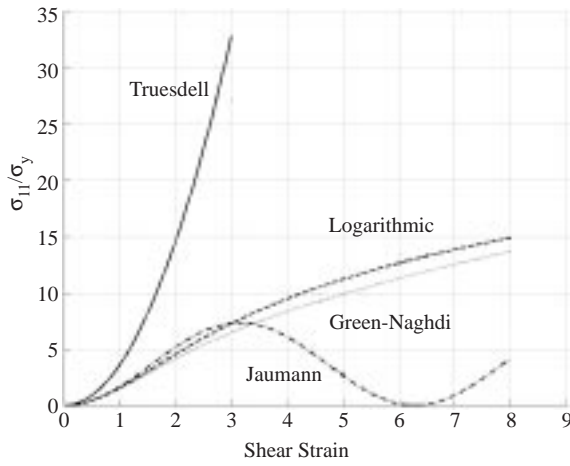


Figure 14. Normal stress vs shear strain: FVBO with zero isotropic stress rate and $E_t = 2000$ MPa.

To model the isotropic hardening using FVBO the isotropic stress is allowed to evolve according to a Frederick-Armstrong type law. At the same time, the kinematic stress is set to zero. Figures 15 and 16 show the simulation results of FVBO with a zero hardening modulus ($E_t = 0$) and a nonzero isotropic stress rate ($\dot{A} \neq 0$). These results are different from the results of the classical plasticity model with isotropic hardening (Figures 5 and 6). In the classical plasticity model, the size of the yield surface, which is represented by the yield strength, grows as a function of the effective inelastic strain rate; see Equations (21) and (24). Since the inelastic rate of deformation tensor continues to evolve during the deformation, the rate of the yield strength will continue to grow and an increasing stress behavior is observed as seen in Figures 5 and 6. On the other hand, in

FVBO isotropic stress has a saturation value and isotropic hardening is observed until the isotropic stress reaches the final value of the isotropic stress A_f , as seen in Figures 15 and 16. Therefore, the simulation results of FVBO with zero hardening modulus ($E_t = 0$) and nonzero isotropic stress rate ($\dot{A} \neq 0$) are similar to the results of FVBO with zero hardening modulus ($E_t = 0$) and zero isotropic stress rate ($\dot{A} = 0$) (Figures 11 and 12) and to the classical plasticity approach with the elastic-perfectly plastic case, (Figures 3 and 4), except the region where the isotropic stress rate is still nonzero.

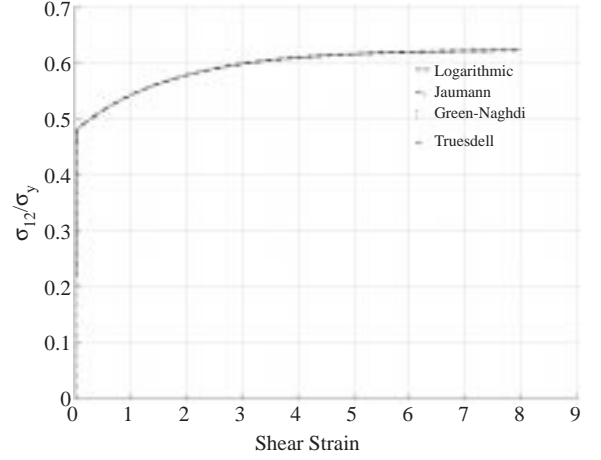


Figure 15. Shear stress vs shear strain: FVBO with $E_t = 0$ and non zero isotropic stress rate ($\dot{A} \neq 0$).

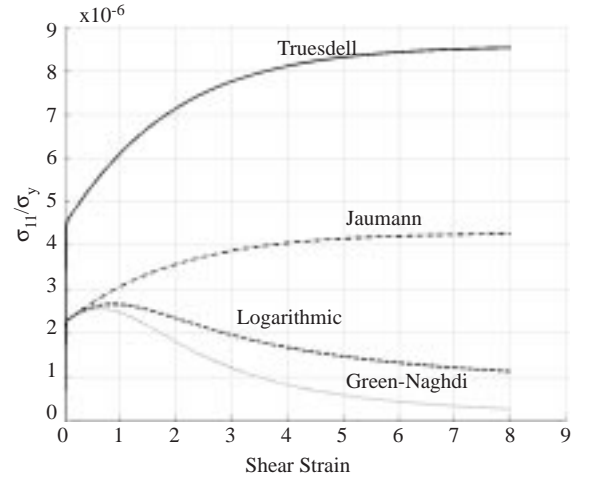


Figure 16. Normal stress vs shear strain: FVBO with $E_t = 0$ and non zero isotropic stress rate ($\dot{A} \neq 0$).

Conclusion

The response under simple shear is investigated using a variety of inelastic material models. Included

are the hypo-elastic, elastic-perfectly plastic, elastic-plastic isotropic and linear kinematic and FVBO, which can be specialized to most of these models. In addition to the well-known Jaumann, Green-Naghdi and Truesdell rates, the influence of the rate newly introduced by Xiao *et al.* (1997a), the logarithmic rate, is also studied for each material model by numerically integrating incremental equations.

The following observations can be made:

1. The responses of the logarithmic rate to every type of model discussed here are acceptable except the elastic-perfectly plastic case. Unlike the Jaumann rate, the logarithmic rate does not exhibit any oscillatory response.
2. FVBO with a zero isotropic stress rate and nonzero hardening modulus and elastic-plastic kinematic hardening model give the same results at the rate of $10^{-5}1/s$.
3. Elastic-plastic kinematic hardening, and elastic-perfectly plastic can be modeled with FVBO.

4. It is reasonable to require that the stresses in simple shear do not develop responses without bounds. However, the material law such as isotropic hardening in plasticity yields the stresses, which have no limit. On the other hand, constant isotropic stress yields finite stresses as the shear strain grows without bounds. If the unlimited growth occurs then the objective derivative is not useful such as the Truesdell rate in Figures 6-8, the Truesdell and Green-Naghdi rates in Figure 13.
5. The choice of stress rate should be governed not only by the principle of objectivity and non-oscillation but also by experimental evidence. However, there are limited experimental data in the literature due to the difficulty in performing simple shear in the laboratory. Therefore, a comparison of the simulation results and experimental data cannot be performed.

References

- Bruhns, O., Xiao, H. and Meyers, A. "Self-consistent Eulerian Rate Type Elasto-Plasticity Models Based Upon the Logarithmic Rate," *International Journal of Plasticity*, 15, 479-520, 1999.
- Colak, O.U. and Krempl, E. "Modeling of Uniaxial and Biaxial Ratcheting Behavior of CS 1026 Carbon Steel Using the Simplified Viscoplasticity Theory Based on Overstress (VBO)," accepted for publication in *Acta Mechanica*, 2002a.
- Colak, O.U. and Krempl, E. "Deformation Induced Anisotropy and the Modeling of The Swift Effect," *Proceedings of the 9th International Symposium on Plasticity*, Plasticity 2002, 310-312, Aruba, Jan. 2002b.
- Colak, O.U. and Krempl, E. "Viscoplasticity Theory Based on Overstress Applied to Cyclic Proportional and Non-proportional Loading," *Proceedings of the 8th International Symposium on Plasticity, Plasticity 2000*, Canada, July, 2000.
- Cotter, B.A. and Rivlin, R.S., "Tensors Associated with Time Dependent Stress", *Q. Appl. Math.*, 13, 177-182, 1955.
- Dafalias, Y.F., "A Missing Link in the Macroscopic Constitutive Formulation of Large Plastic Deformations", In: Sawczuk, A., Bianchi, G. (Eds.), *Plasticity Today*, 135-151, 1985.
- Dienes, J.K., "On the Analysis of Rotation and Stress Rate in Deforming Bodies", *Acta Mech.*, 32, 217-232, 1979.
- Eterovic, A.L., Bathe, K., "A Hyperelastic-Based Large Strain Elasto-Plastic Constitutive Formulation with Combined Isotropic-Kinematic Hardening Using the Logarithmic Stress and Strain Measures", *Int. J. for Numerical Methods in Eng.*, 30, 1099-1114, 1990.
- Green, A.E. and Naghdi P.M., "A General Theory of an Elastic-Plastic Continuum", *Arc. Rat. Mech. Anal.*, 18, 251-281, 1965.
- Johnson, G. and Bammann, D., "Discussion of Stress Rates in Finite Deformation Problems", *Int. J. Solids Structures*, 20, 8, 725-737, 1984.
- Krempl, E., "A Small Strain Viscoplasticity Theory Based on Overstress," In Krausz, A.S., Krausz, K., editors, *Unified Constitutive Laws of Plastic Deformation*, Academic Press, San Diego, 281-318, 1996.
- Krempl, E., "Creep-Plasticity Interaction," *Lecture notes, CISM No: 187*, Udine, Italy, 74, 1998.
- Nagtegaal, J.C. and de Jong J.E., "Some Aspects of Nonisotropic Work Hardening in Finite Strain Plasticity", *Plasticity of Metals at Finite Strain: Theory, Experiment and Computation*, 65, Stanford University Press, 1982.

Oldroyd, J.G., "On Formulation of Rheological Equations of State", Proc. R. Soc. Lond., A200, 523-541, 1950.

Truesdell, C., "The Simplest Rate Theory of Pure Elasticity", Comm. Pure Appl. Math., 8, 123-132, 1955.

Xiao, H., Bruhns, O.T. and Meyers, A., "Logarithmic Strain, Logarithmic Spin and Logarithmic Rate", Acta Mechanica, 124, 89-105, 1997a.

Xiao, H., Bruhns, O.T. and Meyers, A., "Hypo-Elastic Model Based Upon the Logarithmic Stress Rate," Journal of Elasticity, 47, 51-68, 1997b.